Received: August 19, 2020. Revised: November 26, 2020.

INASS

International Journal of
Intelligent Engineering & Systems

http://www.inass.org/

Super-Twisting Second-Order Sliding Mode Control of a Wind Turbine Coupled to a Permanent Magnet Synchronous Generator

Rania Moutchou[1]* Ahmed Abbou[1] Salah Eddine Rhaili[1]

[1]*Mohammadia School of Engineers (EMI), Mohammed V University in Rabat, Morocco*
* Corresponding author's Email: rania.moutchou@um5s.net.ma

Abstract: This paper presents a modelling study and focuses on an advanced higher order slip mode control strategy (Super Twisting Algorithm) for a variable speed wind turbine based on a permanent magnet synchronous generator to capture the maximum possible wind power from the turbine while simultaneously reducing the effect of mechanical stress, powered by a voltage inverter and controlled by vector PWM technique. This paper presents first and second order sliding mode control schemes. On the other hand, a challenging matter of pure SMC of order one can be summed up in the produced chattering phenomenon. In this work, this issue has been mitigated by implementing a new control. The proposed control, characterized by a precision in the case of a continuation of a significant reduction of the interference phenomenon, successfully addresses the problems of essential non-linearity of wind turbine systems. This type of control strategy presents more advanced performances such as behaviour without chattering (no additional mechanical stress), excellent convergence time, robustness in relation to external disturbances (faults in the network) and to non-modelled dynamics (generator and turbine) which have been widely used in power system applications by first order sliding mode control. In particular, second-order sliding regime control algorithms will be applied to the PMSG to ensure excellent dynamic performance. The suggested control is compared to the proportional-integral controller and sliding mode control of order one. The results of simulations under turbulent wind speed and parameter variations show the efficiency, robustness and significantly improved performance of the proposed control approach to distinguish and track quickly (about 10ms depending on the shading pattern) and at the same time saving the main priorities of the sliding mode of order one by reducing the existing chatter. The systems performances were tested and compared using Matlab/Simulink Software.

Keywords: PMSG, Super twisting algorithm, PI, SMC, PWM vector, Wind turbine, Vector control.

1. Introduction

All In addition to other renewable energy sources, wind turbines are one of the fastest growing technologies currently available to generate electricity. Unlike fossil fuel which has risks of scarcity and their effects on climate change, wind power is clean, notably which has been identified as one of the most promising [1, 2]. However, there has been a lot of interest in the methods of operating and developing variable speed wind energy conversion systems (WECS) due to maximizing power extraction energy and increasing efficiency compared to fixed speed [3].

In this article, we focus on variable speed wind turbines which are based on a permanent magnet synchronous generator (PMSG) which offer several advantages such as their high-power density, high efficiency, easy reliability and maintenance [4,5]. In addition, wind turbines should operate efficiently under a wide range of wind speeds; therefore, control designs become more complicated.

The objective of this article is the study of the dynamic behaviour of the synchronous generator with permanent magnet during a speed regulation by classical regulators (PI) and by regulators based on classical sliding mode of order one and of order two (based on the Super Twisting algorithm). However, the control structure using conventional PI type regulators requires precise machine parameters

(changes in internal and external system parameters caused by temperature, humidity and occasional overload will result in loss of stability of regulators conventional). This requires a good identification of the parameters. Therefore, a robust control regulator must be used to maintain acceptable levels of decoupling and performance [3, 4]. The sliding mode control [6, 7] is a nonlinear variable structure control that is robust and efficient in many applications. The control structure changes as a function of the state of the system which is in this case in a steady state, ensuring good performance and robustness with respect to internal and external disturbances and parametric variations, as well as finite time convergence. On the other hand, the state trajectory of the system is brought to a hypersurface called the sliding surface and from this surface it switches to the balance point. The major drawback of first order sliding modes is the appearance of the chattering phenomenon, which is characterized by torque fluctuations [5, 8]. The main cause of this chatter has been identified as the presence of unmodeled parasitic dynamics in the high frequency switching device and additional torsional forces on the generator shaft. This can degrade the performance of mechanical systems and reduces the life of actuators, as well as can drive to system instability [19].

To remedy this problem, another control technique is proposed to transfer the problem of discontinuity due to the switching element of the law in sliding mode on the derivatives of higher order of the variable of sliding, instead of acting on the first derivative as in the case of the first sliding regime state. We are talking about this case of higher order sliding modes (based on the super-twisting algorithm). It then ceases to present the main advantages [17] such as: maintaining the advantages of the sliding state of order one, eliminating the chatter phenomenon and improving the performance of the control in terms of precision.

The article is organized as follows. Section 2 presents a description and a dynamic modelling of PMSG. Section 3 deals with both the design of PI commands and SMC orders of order one and higher and its application to the PMSG in view speed control. Section 4 simulation results performed by means of Matlab/Simulink software are presented and discussed, and then we finish by a conclusion.

Nomenclature:

Sign : Signum function.
SMC : Sliding Mode Controller.
PWM : Pulse Width Modulation.
T : Direct Transformation of PARK.
T^{-1} : Inverse Transformation of PARK.
PI : Proportional-Integral Controller.
WECS: Wind Energy Conversion System.
SMC1: Sliding Mode Controller of order1.
SMC2: Sliding Mode Controller of order1.
PMSG: Permanent Magnet Synchronous Generator.

2. Wind-energy conversion system description

The wind energy conversion system consists of a wind turbine and a PMSG (Fig. 1). A wind turbine is a device that captures the kinetic energy of the wind and converts it into mechanical energy. PMSG is connected to the grid via the grid via a PWM rectifier and a PWM inverter. The generator side control device includes a current control loop and a speed control loop. Due to fluctuations in the power supplied by the generator, a regulation of the DC bus voltage is required via capacitor C.

2.1. Modelling of wind turbine

The aerodynamic power captured by the wind turbine is then [8]:

$$P_a = C_p . P_v \tag{1}$$

$$P_a = \frac{1}{2} . \rho . \pi . R^2 . v^3 . C_p(\Lambda, \beta) \tag{2}$$

Whereρ, S and v represent respectively the density of air, the surface swept by the blades and the wind speed and C_p (λ, β) is the turbine power coefficient.

The power coefficient is defined by the ratio of the power captured by the turbine to the power of the wind (The coefficient C_p represents *the aerodynamic efficiency* of the wind turbine).

$$C_p = \frac{P_a}{P_v} \tag{3}$$

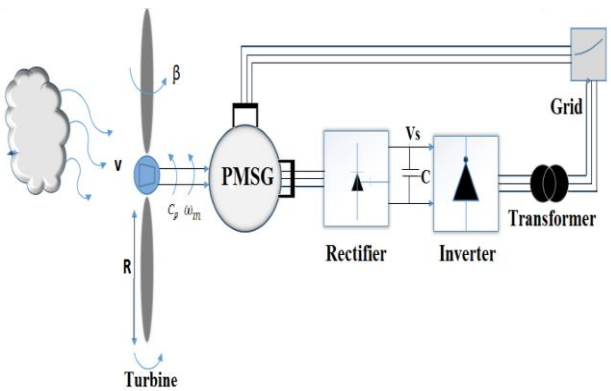

Figure.1 Wind-energy conversion system

According to Betz's law:

$$C_p < 59\% \tag{4}$$

Although its maximum theoretical value is around 0.59, in practice it is between 0.4 and 0.45 [9].

C_p is a function of the specific speed λ and the speed of the wind v defined by [9]:

$$\lambda = \frac{R\Omega}{v} \tag{5}$$

With R the ray of pale of the wind, C_p reactivity power coefficient and Ω the angular a velocity of the turbine.

The power captured by the wind turbine can be expressed by:

$$P_a = \Omega . C_a \tag{6}$$

From the Eq. (6), we can deduce the expression of the aerodynamic torque.

$$C_a = \frac{P_a}{\Omega} \tag{7}$$

From Eq. (2), we obtain:

$$C_a = \frac{1}{2}\frac{\rho.\pi.R^2.v^3.C_p(\lambda,\beta)}{\Omega} \tag{8}$$

With:

$$\Omega = \frac{\lambda v}{R}$$

$$C_a = \frac{1}{2}\frac{\rho.\pi.R^3.v^2.C_p(\lambda,\beta)}{\lambda} \tag{9}$$

We can introduce the torque coefficient:

$$C_T = \frac{C_p}{\lambda} \tag{10}$$

So:

$$C_a = \frac{1}{2}.\rho.\pi.R^3.v^2.C_T(\lambda,\beta) \tag{11}$$

The modelling of the wind torque will therefore depend essentially on taking into account the specificity of the coefficient C_p, since it depends greatly on the type of turbine.

During this work, we have limited ourselves to the case of turbines with a horizontal axis and three blades whose pitch angle is adjustable, which is a standard in current wind turbines.

Asthe expressions for the forces given above show, these increase rapidly with the apparent wind

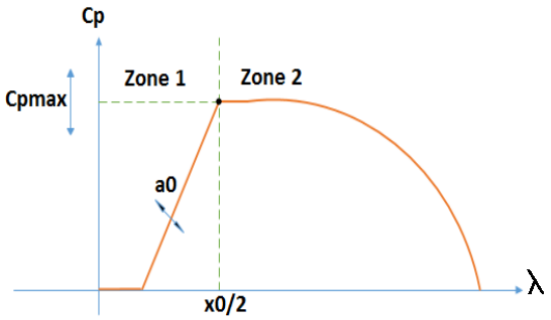

Figure. 2 Power coefficient pace

and the corresponding power can quickly become greater than the nominal power of the generator. It is therefore necessary at a given moment to be able to limit the couple. The adjustment of the latter, and therefore of the power captured by the turbine, is done mainly by action on the lift which depends mainly on the angle of incidence α.

The power coefficient model must take into account the position of the pitch angle which modifies the lift of the blade and therefore makes it possible to control the power captured by the turbine. The general shape of the power coefficient as a function of the speed ratio, for a given pitch angle, is illustrated in (Fig. 2). It is described by Eq. (12) and (13) which respectively represent the parts $\lambda \leq x_0/2$ and $\lambda \geq x_0/2$ [9].

For $\lambda \leq x_0/2$:

$$C_p(\lambda,\beta) = C_{pmax}(\beta)\frac{(-4)}{x_0(\beta)^2}\lambda(\lambda - x_0(\beta))e^{-\frac{(\lambda-\frac{x_0(\beta)}{2})^2}{a_0}} \tag{12}$$

a_0 is the slope of the curve.

For $\lambda \geq x_0/2$:

$$C_p(\lambda,\beta) = C_{pmax}(\beta)\frac{(-4)}{(2x_1(\beta)-x_0(\beta))^2}[(\lambda - x_1(\beta))\left(\lambda(x_0(\beta)-x_1(\beta))\right) \tag{13}$$

We choose a parabolic law for $x_0(\beta)$:

$$x_0(\beta) = 2\lambda_0 + \frac{8}{\beta_{max}^2}(\lambda_{max}-\lambda_{opt})\beta(\beta_{max}-\beta) \tag{14}$$

$$x_1(\beta) = \frac{(x_1)_0}{(x_0)_0}x_0(\beta) \tag{15}$$

$$C_{pmax}(\beta) = C_{PMAX} - \Delta C(\beta - b\beta^{\alpha}) \qquad \alpha > 1$$

C_{PMAX} is the max of C_{pmax} (β), b a model parameter to be adjusted.

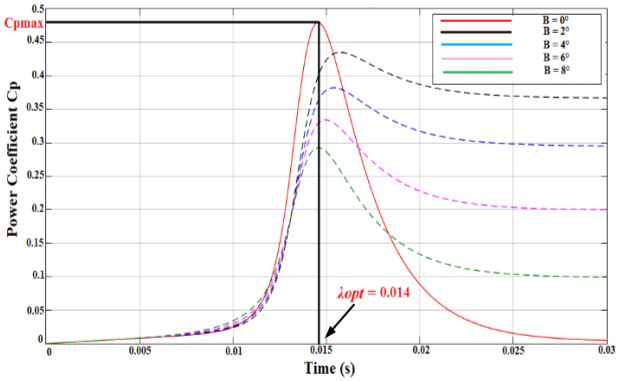

Figure. 3 Power coefficient C_p for different values of the setting angle β as a function of the speed ratio λ

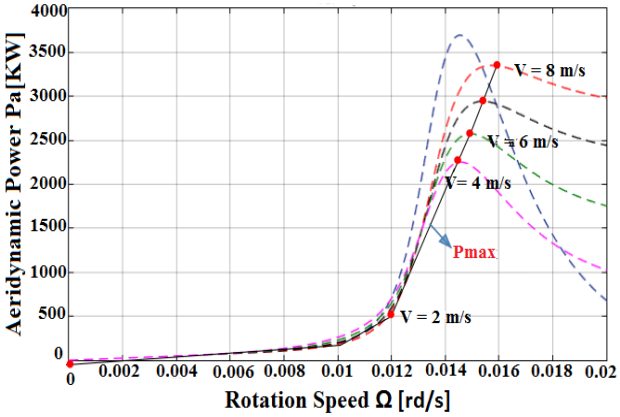

Figure. 4 Power captured by the turbine for a different wind speed of as a function of the rotation speed Ω and for a zero setting angle β

The maximum value of C_p (C_{pmax}= 0.48) achieved for λ=0.014 and β= 0 is illustrate in (Fig. 3).
In (Fig. 4), the captured power P_a for a wind turbine is shown as a function of the turbine rotation speed Ω, for a different wind speed value and for a setting angle β= 0 [9].
Expression of the aerodynamic torque is equal to the torque of the fast shaft:

$$C_a = C_g \tag{16}$$

By taking into account the coefficients of stiffness and damping, the expression of the dynamics of the turbine is expressed by [13]:

$$J\Omega = C_a - f\dot{\Omega} - B\theta - C_{mec} \tag{17}$$

Ω and J represent respectively the mechanical speed and moment of inertia, B shaft stiffness coefficient, θ slow shaft angle and C_{mec} tree couple.
Since the stiffness is very low, it can be neglected. The fundamental equation of dynamics can be written:

$$C_{mec} = C_g - C_{em} - f\Omega \tag{18}$$

Where, C_{em} is the electromagnetic torque and f is a viscous friction coefficient.

2.2. PMSG modelling

Taking into account the simplifying assumptions, we used the Park transformation to model the PMSG, the goal of which is to make the impedance matrix independent.
The electrical equations then give the following system:

$$\begin{cases} v_d = L_s \frac{di_d}{dt} + R_s i_d - L_s \omega_r i_q \\ v_q = L_s \frac{di_q}{dt} + R_s i_q + p\omega_r i_d \end{cases} \tag{19}$$

R_s resistance of the stator winding, L_d the direct inductance of the stator winding, L_q inductance in squaring of the stator winding.
In any two-phase reference, the active and reactive stator powers of a synchronous generator are written as follows:

$$\begin{cases} P_s = v_d i_d + v_q i_q \\ Q_s = v_q i_d - v_d i_q \end{cases} \tag{20}$$

The adaptation of these equations to the chosen system of axes and to the simplifying assumptions considered in our case gives:

$$\begin{cases} v_d = 0 \\ v_q = v_s \end{cases} \tag{21}$$

$$\begin{cases} P_s = v_s i_q \\ Q_s = v_s i_d \end{cases} \tag{22}$$

The electromagnetic torque can be expressed as a function of the stator flux and current:

$$C_{em} = \frac{3}{2} p[(L_d - L_q) i_d i_q + f i_q \emptyset] \tag{23}$$

3. Control system

3.1. Sliding mode control design

The implementation of this control method to the PMSG requires mainly three stages:
J. Slotine proposed a general equation to determine the sliding surface [8].

$$S(x,t) = \left(\frac{d}{dt} + \lambda\right)^{n-1} e(t) \tag{24}$$

With λ is a positive coefficient.
The adjustment error is chosen as the surface:

$$e(t) = x_{ref}(t) - x(t) \quad (25)$$

So: $$e(t) = w_{rref} - w_r \quad (26)$$

For n=1, the rotational speed equation can be obtained from Eq. (24) as follows:

$$S(\dot{w_r}) = \dot{w_{rref}} - \dot{w_r} \quad (27)$$

With:

$$\dot{S}(w_r) = \dot{w_{rref}} - \frac{p(L_d - L_q)\iota_d - p\dot{\emptyset}_f \iota_q}{J} + \frac{1}{f}C_r - \frac{f}{J}w_r \quad (28)$$

The convergence condition is defined by the equation of Lyapunov [3]:

$$S(w_r)\dot{S}(w_r) < 0 \quad (29)$$

If replacing Eq. (29) in (28), we obtain:

$$\dot{S}(w_r) = -[\frac{p(L_d - L_q)}{J} i_d - p\emptyset_f] i_{qN} \quad (30)$$

The structure of the controller consists of two parts: the first involves precise linearization, and the second involves stabilization.

$$i_q = i_{qeq} + i_{qN} \quad (31)$$

i_{qeq} is the equivalent command suggested, it is described by [3]:

$$\dot{S}(w_r) = 0 \quad (32)$$

$$i_{qN} = -Ksign(S(w_r)) \quad (33)$$

Where: K > 0; K is the control gain.

We have:

$$i_{qN} = 0 \quad (34)$$

$$sign\big(S(w_r)\big) = \begin{cases} 1 & S(w_r) > 0 \\ 0 & S(w_r) = 0 \\ -1 & S(w_r) < 0 \end{cases} \quad (35)$$

Fig. 5 shows the scheme of the sliding mode setting of order 1 (SMC1), using the principle of the cascade control method (three-surface structure).

The direct current error e_d is chosen as:

$$e_d = i_{dref} - i_d \quad (36)$$

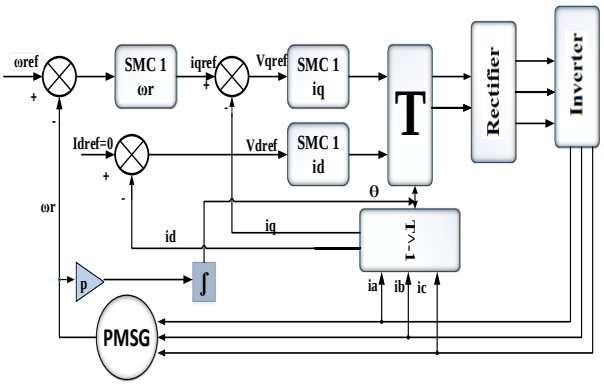

Figure. 5 Diagram block of sliding mode control of order 1

The sliding surface of the current i_d is defined from Eq. (24):

$$S(i_d) = i_{dref} - i_d \quad (37)$$

$$S(\dot{i_d}) = \iota_{d\dot{r}ef} - \dot{i_d} \quad (38)$$

We obtain:

$$S(\dot{i_d}) = \iota_{d\dot{r}ef} - \frac{R_s}{L_d} i_d + p\omega_r \frac{L_q}{L_d} i_q + \frac{1}{L_d} V_d \quad (39)$$

The control voltage V_{deq} and V_{dN} commands are defined by:

$$V_{deq} = \left[\iota_{d\dot{r}ef} - \frac{R_s}{L_d} i_d - \frac{PL_q w_r}{d} i_q\right] L_d \quad (40)$$

$$V_{dN} = K_d sign\,(S(i_d)) \quad (41)$$

Where:

K_d: Positive constant.

The quadrature current error e_q is chosen as:

$$e_q = i_{qref} - i_q \quad (42)$$

The sliding surface of the current i_q is defined from Eq. (24):

$$S(i_q) = i_{qref} - i_q \quad (43)$$

$$S(\dot{i_q}) = \iota_{q\dot{r}ef} - \dot{i_q} \quad (44)$$

We obtain:

$$S(\dot{i_q}) = \iota_{q\dot{r}ef} - \frac{R_s}{L_q} i_d - \frac{1}{L_q} p\omega_r i_d + \frac{1}{L_q} V_q \quad (45)$$

The control voltage V_{qeq} and V_{qN} commands are defined by:

$$V_{qeq} = \left[\dot{\iota_{qref}} - \frac{R_s}{L_q} p w_r i_d + \frac{P\emptyset_f}{L_q} \right] q \quad (46)$$

$$V_{qN} = K_q sign\,(S(i_q)) \quad (47)$$

Where:
K_q: Positive constant.

3.2 Super-twisting sliding mode control design

3.2.1. Super-twisting algorithm

The super-twisting algorithm is developed for a system with a relative degree of 1, to avoid jitter in a system with variable structure [17].

The convergence of this algorithm is also governed by the rotations around the origin of the phase diagram. The control u(t) as a sum of two components. The first is defined by its derivative with respect to time (u_1), while the second is given by the continuous function of the sliding variable (u_2):

$$u(t) = u_1(t) + u_2(t) \quad (48)$$

$$\dot{u_1}(t) = \begin{cases} -u & if\ |u| > U \\ -W sign(S) & if\ |u| \le U \end{cases} \quad (49)$$

Where |u| is a bounded command value, given for $|u| \le 1$.

$$u_2(t) = \begin{cases} -\lambda_1 |S_0|^{\rho_1} sign(S) & if\ |S| > S_0 \\ -\lambda_1 |S|^{\rho_1} sign(S) & if\ |S| \le S_0 \end{cases} \quad (50)$$

The sufficient condition of limited time convergence is [18]:

$$\begin{cases} W > \frac{\emptyset}{\Gamma_{min}} \\ \lambda_1^2 > \frac{4\emptyset\Gamma_{max}(W+\emptyset)}{\Gamma_{min}^2 \Gamma_{min}(W-\emptyset)} \\ 0 < \rho_1 < 1/2 \end{cases} \quad (51)$$

There is a positive constant (Φ, Γ_m, S_0) as in the region $|S| \le S_0$.
$\Gamma_{min} = 0.651$ and $\Gamma_{max} = 0.977$ a positive constant.

The gains of Super-twisting sliding mode controller of Eq. (50) are designed a $\lambda = 60$ and W = 80. The sliding surface slope is 4, which is same as that of the conventional sliding mode controller. The equivalent controller is:

$$u_{eq}(t) = 190u_1(t) - 5{,}12u_2(t) \quad (52)$$

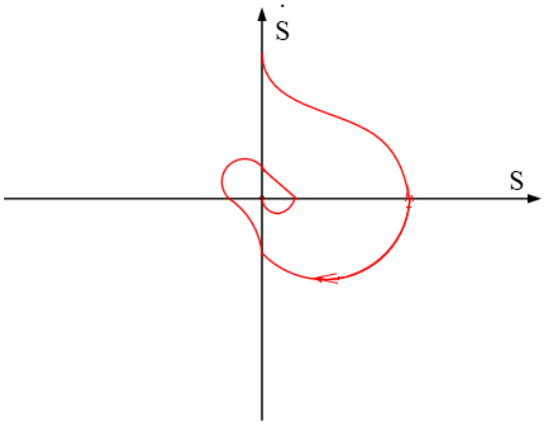

Figure. 6 Convergence en temps fini de l'algorithme twisting

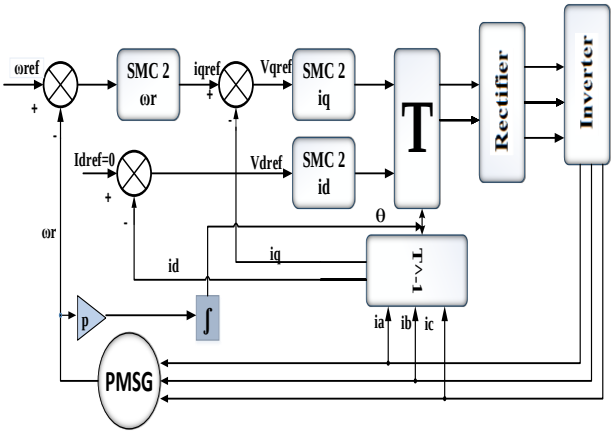

Figure. 7 Diagram block of sliding mode control of order 2

The state trajectory of the phase plane is shown in (Fig. 6). It twists in the state space and approaches the origin. Finally, it converges to the origin of the phase plane.

3.2.2. Application of the command to the PMSG

The diagram of the order by sliding order 2 is shown in (Fig. 7). Using the principle of the cascade adjustment method (structure of three surfaces), the internal loop makes it possible to control the currents, while the external loop makes it possible to control the speed.

At this point, in order to achieve the required control objective during sliding mode operation, the sliding variable can be selected as:

$$\begin{cases} S_1 = \omega_{rref} - \omega_r \\ S_2 = i_{qref} - i_q \\ S_3 = i_{dref} - i_d \end{cases} \quad (53)$$

For a relative degree equal to one (r=1), the Super Twisting control law is as follows:

$$\begin{cases} u_i = -\lambda_i |S_i|^{\frac{1}{2}} sign(S_i) + u_{1i} \\ \dot{u_{1\iota}} = -W_\iota sign(S_i) \\ and\ i = 1,2,3 \end{cases} \quad (54)$$

Where $W_i = kw_r$.

The dynamic modelling of the permanent magnet synchronous generator rotating reference frame can be expressed as follows [13]:

$$\frac{di_d}{d\tau} = -\frac{R_S}{L_d} i_d + \frac{L_q}{L_d} p\omega_r i_q - \frac{1}{L_d} u_d \quad (55)$$

$$\frac{di_q}{d\tau} = -\frac{R_S}{L_q} i_q + \frac{L_d}{L_q} p\omega_r i_d - \frac{\emptyset_f}{L_q} p\omega_r - \frac{1}{q} u_q \quad (56)$$

$$\frac{d\omega_r}{d\tau} = -\frac{3p}{2J}\left[\left(L_d - L_q\right) i_d i_q + f\emptyset_f i_q\right] - \frac{f}{J}\omega_r \frac{1}{J} C_r \quad (57)$$

3.2.3. D-axis controller design

The goal of the d-axis controller is keeping the d-axis current of the generator to zero, both s(x) and ṡ(x) must be zero, so one more derivative of each function must be calculated. From the previous equation, we have [14]:

$$\dot{s_d} = \frac{1}{L_d}\left[-R_s \iota_d + p\omega_r L_d L_q - u_d\right] - \frac{d\iota_{dref}}{dt} \quad (58)$$

From Eq. (58), $\ddot{s}_d$ is found to be:

$$\ddot{s_d} = -\frac{R_s}{L_d}\frac{di_d}{dt} + p\frac{d\omega_r}{dt} i_q + p\frac{di_q}{dt}\omega_r - \frac{1}{L_d}\frac{du_d}{dt} - \frac{d^2 i_{dref}}{dt^2} \quad (59)$$

The control input u_d consists of the sum of u_{deq} the equivalent control, and $\tilde{u}_d$ is defined as:

$$\widetilde{u_d(t)} = u_{d1}(t) + u_{d2}(t) \quad (60)$$

According to (60), we can use super-twisting sliding mode control. Hence, the unknown term of the d-axis controller can be expressed by:

$$\dot{u_{d1}} = -W_d sign(S_d) \quad (61)$$

$$u_{d2}(t) = \begin{cases} -\lambda_1 |S_0|^{\rho_1} sign(\dot{S_d}) & if\ |S_d| > S_0 \\ -\lambda_1 |S_d|^{\rho_1} sign(S_d) & if\ |S_d| \le S_0 \end{cases} \quad (62)$$

$$\begin{cases} W_d > \frac{\emptyset_d}{\Gamma_{min}} \\ \lambda_1^2 > \frac{4\emptyset_d \Gamma_{max}(W_d + \emptyset_d)}{\Gamma_{min}^2 \Gamma_{min}(W_d - \emptyset_d)} \\ 0 < \rho_1 < 1/2 \end{cases} \quad (63)$$

We have:

$$\widetilde{u_d} = -\lambda_1 |S_d|^{\frac{1}{2}} sign(S_d) - W_d \int sign(S_d) dt \quad (64)$$

As a result, d-axis control law becomes:

$$u_d = u_{deq} + \widetilde{u_d} \quad (65)$$

3.2.4. Q-axis controller design

The same method used for the direct axis is applied to the quadrature axis. Previously,

$$\dot{s_q} = \frac{1}{L_q}\left[-R_s i_q + p\omega_r\left(L_d i_d - \emptyset_f\right) - u_q\right] - \frac{di_{qref}}{dt} \quad (66)$$

From Eq. (66), $\ddot{s}_q$ is found to be:

$$\ddot{s_q} = -\frac{R_s}{L_q}\frac{di_q}{dt} + p\left(i_q - \frac{\emptyset_f}{L_q}\right)\frac{d\omega_r}{dt} + p\frac{di_d}{dt}\omega_r - \frac{1}{L_q}\frac{du_q}{dt} - \frac{\boldsymbol{d^2 i_{qref}}}{\boldsymbol{dt^2}} \quad (67)$$

The control input u_q consists of the sum of u_{qeq} the equivalent control, and $\tilde{u}_q$ is defined as:

$$\widetilde{u_q(t)} = u_{q1}(t) + u_{q2}(t) \quad (68)$$

According to (68), we can use super-twisting sliding mode control. Hence, the unknown term of the q-axis controller can be expressed by:

$$\dot{u_{q1}} = -W_q sign(S_q) \quad (69)$$

$$u_{q2}(t) = \begin{cases} -\lambda_1 |S_0|^{\rho_1} sign(\dot{S_q}) & if\ |S_q| > S_0 \\ -\lambda_1 |S_q|^{\rho_1} sign(S_q) & if\ |S_q| \le S_0 \end{cases} \quad (70)$$

$$\begin{cases} W_q > \frac{\emptyset_q}{\Gamma_{min}} \\ \lambda_1^2 > \frac{4\emptyset_q \Gamma_{max}(W_q + \emptyset_q)}{\Gamma_{min}^2 \Gamma_{min}(W_q - \emptyset_q)} \\ 0 < \rho_1 < 1/2 \end{cases} \quad (71)$$

We have:

$$\widetilde{u_q} = -\lambda_1 |S_q|^{\frac{1}{2}} sign(S_q) - W_q \int sign(S_q) dt \quad (72)$$

As a result, q-axis control law becomes:

$$u_q = u_{qeq} + \widetilde{u_q} \quad (73)$$

3.2.5. Q-axis current reference controller design

From the previous Eq. (28), $\dot{s}_{wr}$ is found to be:

$$\ddot{s_{\omega_r}} = -\frac{C_r}{J} - k_t\left(\frac{di_d}{dt}i_q + \frac{di_q}{dt}i_d\right) - k_f\frac{di_q}{dt} - \frac{f}{J}\frac{d\omega_r}{dt} - \frac{d^2\omega_{rref}}{dt^2} \quad (74)$$

Where: $k_t = \frac{3}{2}p(L_d - L_q)$ and $k_f = \frac{3}{2}pf\emptyset_f$

The control input i_q consists of the sum of i_{qeq} the equivalent control, and $\tilde{i}_q$ is defined as:

$$\widetilde{i_q(t)} = i_{q1}(t) + i_{q2}(t) \quad (75)$$

According to (75), we can use super-twisting sliding mode control. Hence, the unknown term of the d-axis controller can be expressed by:

$$\dot{\imath_{q1}} = -W_{\omega_r} sign(S_{\omega_r}) \quad (76)$$

$$i_{q2}(t) = \begin{cases} -\lambda_1|S_0|^{\rho_1} sign(\dot{S}_{\omega_r}) & if\ |S_{\omega_r}| > S_0 \\ -\lambda_1|S_{\omega_r}|^{\rho_1} sign(S_{\omega_r}) & if\ |S_{\omega_r}| \le S_0 \end{cases} \quad (77)$$

$$\begin{cases} W_{\omega_r} > \frac{\emptyset_{\omega_r}}{\Gamma_{min}} \\ \lambda_1^2 > \frac{4\emptyset_q\Gamma_{max}(W_{\omega_r}+\emptyset_{\omega_r})}{\Gamma_{min}^2\Gamma_{min}(W_{\omega_r}-\emptyset_{\omega_r})} \\ 0 < \rho_1 < 1/2 \end{cases} \quad (78)$$

We have:

$$\dot{\tilde{\imath_q}} = -\lambda_1|S_{\omega_r}|^{\frac{1}{2}} sign(S_{\omega_r}) - W_{\omega_r}\int sign(S_{\omega_r})dt \quad (79)$$

As a result, q-axis control law becomes:

$$i_q = i_{qeq} + \tilde{i_q} \quad (80)$$

4. Simulations results

In this section, we will test the performance of the different controllers presented in the previous section. To evaluate the performances of designed super-twisting sliding mode control in the PMSG-based wind turbines, the several simulations have been carried out on the MATLAB/ Simulink software [15, 16]. The system parameters are listed in Tables 1 and 2.

Dynamic performances

The modelling of the wind profile requires climatic and geographical data of the concerned site,

Table 1. Turbine parameters

Blade radius	R=50
Power Coefficient	Cpmax=0.48
Optimal relative wind speed	λopt=0.014
Mechanical speed multiplier	B=87.4
Moment of inertia	J=0.0014kgm^2
Damping coefficient	f=0.0050 N ms/rad
Density of air	ρ=1.2
Rated rotational speed	$\omega_r = 314$ rad/s

Table 2. PMSG parameters

Rated Power	1.5MW
Rated stator voltage	Vs=76.2V
Nominal frequency	F=50Hz
Number of pole pair	p=6
Stator Resistance	Rs=0.0083Ω
Stator Inductance	Ls=0.00331H
Direct Inductance	Ld=0.017 H
Quadrature Inductance	Lq=0.017H
Load torque	$C_r = 10$ N. m
Flux	Φ = 2 Wb

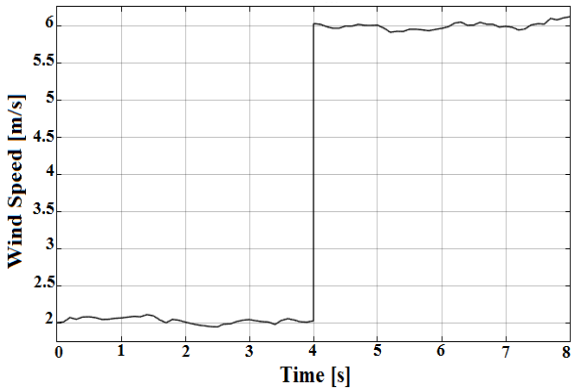

Figure. 8 Wind speed (m/s)

Fig. 9 and Fig. 10 shows the speed of rotation and torque of the PMSG in the case of a no-load start for a speed. The influence of the wind speed on the speed of rotation of the turbine, as well as the electromagnetic torque. All these quantities are of the same form because of the linear relationship that exists between them.

Fig. 11 and Fig. 12 shows the shape of the direct currents i_d and the quadrature current i_q respectively, where the direct current has the same form as the quadrature current while it is negative.

We have reversed the direction of rotation from +100 rad/s to -100 rad/s at time t = 0.1s without load. The simulation results show that the speed perfectly follows its reference which is reached very quickly. The error caused by the load disturbance is instantly compensated. The reversal of the direction of rotation makes it possible to deduce that the control is robust.

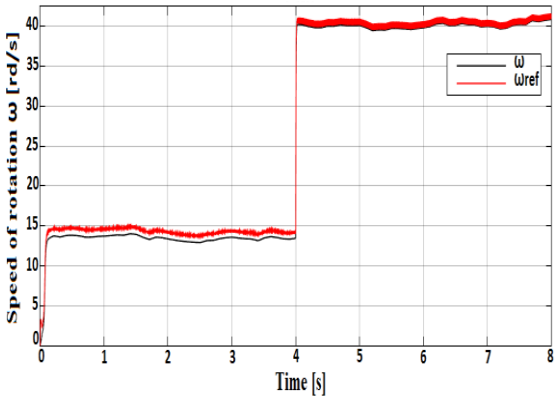

Figure. 9 Speed of rotation ω

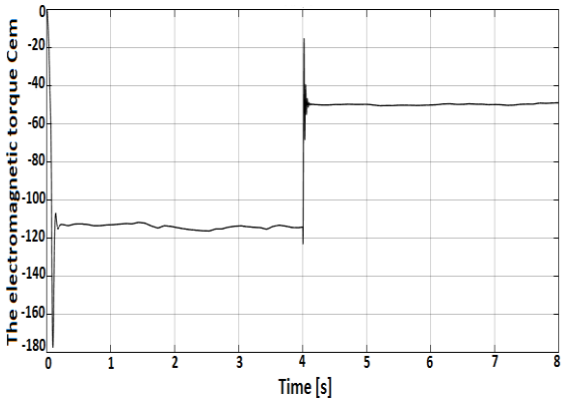

Figure. 10 The torque cem

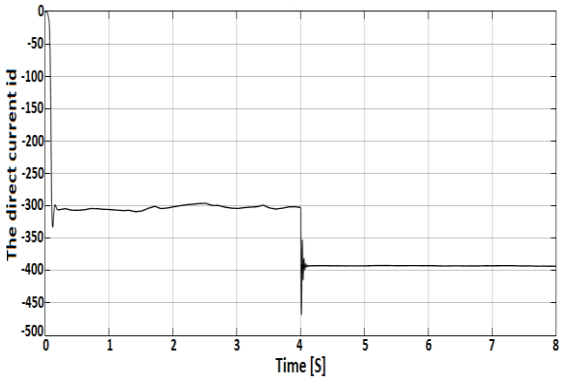

Figure. 11 The direct currents id

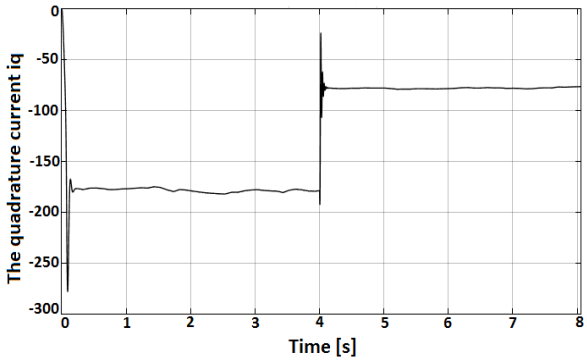

Figure. 12 The quadrature current iq

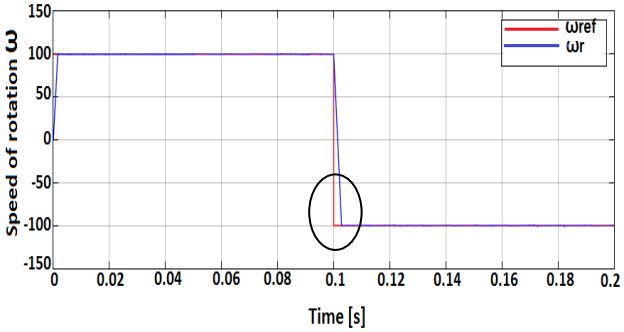

(a)

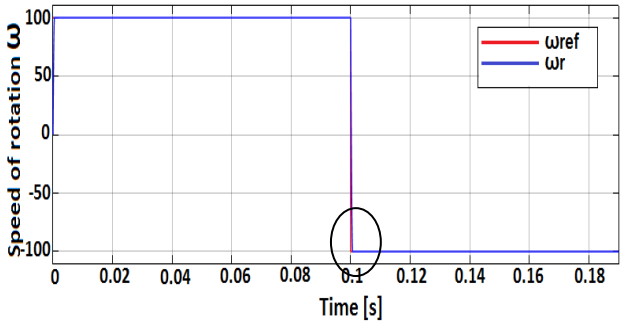

(b)

Figure. 13 Simulation results for a variation of the reference speed of rotation ω: (a) SMC1 and (b) SMC2

Comparative Study between SMC1 and SMC2

The comparison of the speed and the torque of the PMSG is made for a reference speed of 100 rad/s, and followed by a load application of 5 N.m at the instant t = 0.1s.

Speed of rotation ω

In Fig13, we have reversed the direction of rotation from +100 rad / s to -100 rad / s at time t = 0.1s without load. The simulation results show that the speed of SMC2 perfectly follows its reference without overshoot in a very short response time compared to the SMC1. The application of the load shows almost no influence on the pace of speed. Reversing the direction of rotation makes it possible to deduce that the control is robust.

The electromagnetic torque C_{em}

Fig. 14 shows that the response of the electromagnetic torque in the control case is compared. It is clear that the regulator SMC2 using the super twisting algorithm reduces the chatter existing in the case of SMC1. The torque undergoes a peak at the time of starting, and then quickly reaches the resistance torque value before and after the application of the load. The error caused by the disturbance of the load is instantly compensated.

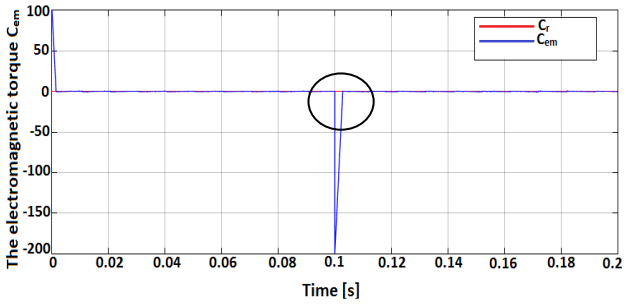

(a)

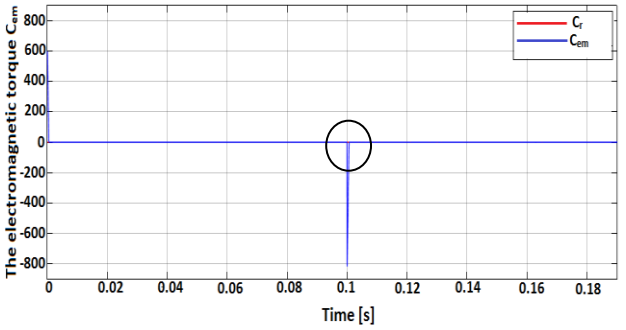

(b)

Figure. 14 Simulation results for a variation of the torque C_{em}

5. Conclusion

This work shows the technique of higher order sliding mode control. In the first place we have given in detail the main sliding order command algorithm of two, such as Super Twisting which is the most used in the literature. The advantage of this method lays in the fact that it can be applied to a system to a relative degree greater than two. It discusses a variable structure control method (SMC2) of the PMSG in a cascade structure. We have defined the necessary design methodology for this control for speed control.

The simulation results show that the responses of SMC2 based on the super twisting algorithm for speed control are fast and robust during variations in load or speed.

The basic principle and the design procedure of super-twisting sliding mode control are discussed. Super-twisting sliding mode control is a second order sliding mode control scheme which eliminates the chattering effect without degrading the transient response, steady-state response and robustness. However, the performance of super-twisting sliding mode control heavily depends on the sliding surface. If the sliding surface is designed properly, super-twisting sliding mode control can eliminate the chattering effect without degrading the tracking performance and robustness. If the sliding surface is not designed properly, it may lead to adverse effects in the response, which are not desirable.

Finally, a comparative study between SMC2 and SMC1 from PMSG was presented. The SMC2 controller is faster, we see that the speed perfectly follows its reference which is reached very quickly for 0.1 s while the SMC1 controller follows for 0.11s, this shows the efficiency of Super-Twisting. When reversing, the speed decreases due to the operation of the machine as a generator delivering a resistant electromagnetic torque which serves to break the machine. Then when the rotation reverses the machine runs as a motor, the speed increases until it reaches its new benchmark of -100 rad / s. So we can say that the robustness of this command is guaranteed with respect to this operation. The advantage of SMC2 based on the super twisting algorithm is translated by the reduction of chatter and at the same time saving the main priorities of the sliding mode of simple order.

For the continuity of the research relating to this work, we propose as perspectives the implementation of the commands presented in the external card in order to verify and validate in real time the results found.

Symbols List	
P_a	The aerodynamic power
C_p	Power coefficient
P_v	The wind turbine
ρ	Air mass density
R	Turbine Radius (m)
v	The wind speed (m/s)
Ω	The angular velocity of the turbine
C_a	The aerodynamic torque
C_T	The torque coefficient
β	The blade pitch angle
C_{pmax}	Power coefficient maximum
C_g	The torque of the fast shaft
J	The total moment of inertia
F	Grid frequency
S	Sliding Surfaces
f	The viscous friction coefficient
θ	Slow shaft angle
C_{mec}	Mechanical torque
C_{em}	Electromagnetic torque
C_r	The resistant torque
v_d,v_q	The stator dq-axis voltages
i_d,i_q	The stator dq-axis currents components
L_s	Stator inductance
$L_{d,q}$	The stator dq-axis inductances
R_s	The stator resistance
V_s	The stator voltage

ω_r	Generator speed
ω_m	Mechanical speed
p	The number of the poles
P_s	The active power
Q_s	The reactive power
Φ	The permanent magnet flux
ω_{rref}	The reference Generator speed
i_{dref}	The reference direct current
i_{qref}	The reference quadrature current
e	Steady state error
i_N	The current of SMC
k	Positive gain of SMC
u	The control component
$u_{d,q}$	The dq-axis control
$S_{d,q}$	The dq-axis positive constant
k_d,k_q	Positive gain of SMC1
k_t,k_f	Positive gain of SMC2
ρ_1	The maximum real sliding order two
i	The WECS fixed drive train multiplying ratio
S_0, W, U, Φ	Positive constant of machine side switching efforts
Γ_{min}, Γ_{max}	Positive constant
C	Capacitor

References

[1] N. Khemiri, A. Khedher, and M. Faouzi. "Wind Energy Conversion System using DFIG Controlled by Backstepping and Sliding Mode Strategies", *International Journal of Renewable Energy Research*, Vol.2, No.3, 2012.

[2] E. Mahersi, A. Khedher and M. F. Mimouni, "TheWindenergy Conversion System Using PMSG Controlled by Vector Control and SMC Strategies", *International Journal of Renewable Energy Research*, Vol. 2, No. 4, pp. 732-741, 2012.

[3] R. Moutchou and A. Abbou, "Comparative Study of SMC and PI Control of a Permanent Magnet Synchronous Generator Decoupled by Singular Perturbations", In: *Proc. of 7th International Renewable and Sustainable Energy Conference*, 2019

[4] Q. Wang, H. Yu, M. Wang, and X. Qi, "A Novel Adaptive Neuro-Control Approach for Permanent Magnet Synchronous Motor Speed Control", *Energies*, Vol. 11, No. 9, 2018.

[5] S. Rhaili, A. Abbou, S. Marhraoui, R. Moutchou and N. El Hichami, "Robust Sliding Mode Control with Five Sliding Surfaces of Five-Phase PMSG Based Variable Speed Wind Energy Conversion System", *International Journal of Intelligent Engineering and Systems*, Vol.13, No.4, pp. 346-357, 2020.

[6] B. Beltran, M. E. H. Benbouzid, and T. Ahmed-Ali, "Second-Order Sliding Mode Control of a Doubly Fed Induction Generator Driven Wind Turbine", *IEEE Transactions on Energy Conversion*, Vol. 27, No. 2, pp. 261-269, 2012.

[7] P. Gajewski and K. Pieńkowski, "Analysis of Sliding Mode Control of variable speed wind turbine system with PMSG", In: *Proc. of International Symposium on Electrical Machines*, Naleczow, Poland, pp. 1-6, 2017

[8] G. Zhuo, J. Hostettler, P. Gu, and X. Wang, "Robust Sliding Mode Control of Permanent Magnet Synchronous Generator-Based Wind Energy Conversion Systems", *Sustainability*, Vol. 8, No. 12, pp. 1-20, 2016.

[9] R. Moutchou and A. Abbou, "MPPT and Pitch Angle Control of a Permanent Magnet Synchronous Generator based Wind Emulator", *International Journal of Innovative Technology and Exploring Engineering*, Vol. 8, No. 7, 2019.

[10] V. Kumar, S. R. Mohanty, and S. Kumar, "Event Trigger Super Twisting Sliding Mode Control for DC Micro Grid with Matched/UnmatchedDisturbanceObserver", *Sm art Grid IEEE Transactions on*, Vol. 11, No. 5, pp. 3837-3849, 2020.

[11] S. Shoja-Majidabad, H. Toosian-Shandiz, and A. Hajizadeh, "Robust fractional-order control of PMSG-based WECS", *Int. J. Autom. Control*, Vol. 9, No. 2, pp. 107-129, 2015.

[12] B. Abdelouaheb, "Contribution à la commande adaptative floue pour les systèmes non linéaires discrets incertains", *Thèse de Doctorat, Université Ferhat ABBAS Sétif-1*, 2019.

[13] R. Moutchou, A. Abbou, and A. vall Hemeyine "Control of the Active and Reactive Powers of a Permanent Magnet Synchronous Generator Decoupled by Singular Perturbations", In: *Proc. of the 9th International Renewable Energy Congress*, 2018.

[14] A. A. Z. Diab, A. A. Ahmed, and H. A. Abdelsalam, "Fuzzy-based Adaptive Sliding Mode Control for a Direct-Driven PMSG Wind Energy System", In: *Proc. of the 21st International Middle East Power Systems Conf.*, Cairo, pp. 81-88, 2019.

[15] M. Nasiri, J. Milimonfared, and S. H. Fathi, "A review of low voltage ride-through enhancement methods for permanent magnet synchronous generator based wind turbines", *Renewable &*

Sustainable Energy Reviews, Vol. 47, pp. 399–415, 2015.

[16] M. Nasiri, J. Milimonfared, and S. H. Fathi, "Robust control of PMSG-based wind turbine under grid fault conditions", *Indian Journal of Science and Technology*, Vol. 8, No. 13, 2015.

[17] I. Deghboudj, "Commande des systemes non lineaires par mode glissant d'ordre superieur", *Thèse de Magister, Université de Constantine 1*, 2013.

[18] J. K. Goyal, S. Kamal, R. B. Patel, X. Yu, J. P. Mishra, and S. Ghosh, "Higher Order Sliding Mode Control-Based Finite-Time Constrained Stabilization", *Circuits and Systems II: Express Briefs IEEE Transactions on*, Vol. 67, No. 2, pp. 295-299, 2020.

[19] I. Deghboudj, "Commande des systemes non lineaires par mode glissant d'ordre superieur", *Thèse de Magister, Université de Constantine 1*, 2013.